

Appendix III

Classifications of ALTR/ARMD

Two main classifications for the ALTR/ARMD have been used with the intent of providing a grading system of severity for clinical purposes [1,2], where other authors have preferred grading features of the reactions [3-6], aware of the limited value of any classification with a rationale similar to the one used by some researchers for MRI evaluation [7]. A recent report has concluded that the current pathologic scoring systems for ALTR/ARMD are not reproducible [8] and it has been accepted as evidence in a commentary to the study [9]. Since the authors suggest that the results of several publications should be interpreted with caution because of unreported intraclass correlation coefficient (ICC), we examined the individual case score sheet for each pathologist provided by the authors and found several cases with differences greater than 1 point in any scoring category of the two classifications examined [1, 2], which are unusual for experienced pathologists in the field. The differences found in the scoring of presence or absence of specific cell types in the Oxford classification among the three examining pathologists were also not consistent with a comparable degree of expertise or accuracy of the examination of the histological slides. Therefore, appropriate statistical analysis was performed, and the results reported in Appendix IV indicate a difference in expertise or accuracy of the examination among the three pathologists rather than lack of reproducibility of the proposed classifications.

Four major histological patterns of ALTR/ARMD have been consistently reported in the literature with only minor differences and their features are summarized in [Table 1](#).

Table 1 Histological patterns of ALTR/ARMD.

| Histological Pattern | Characteristics |
|---|--|
| 1. Macrophage w/wo Bone Infiltration (Osteolysis) | Macrophage infiltrate (grade ≥ 1) without or with minimal evidence of interstitial and/or perivascular lymphocytic infiltrate (<grade 1) |
| 2. Mixed Macrophage and Lymphocytic w/wo Plasmacytic Component w/wo Bone Infiltration (Osteolysis) | Macrophage (grade ≥ 1) and lymphocytic (grade ≥ 1) infiltrate |
| 3. Predominant Lymphocytic with Variable Macrophage Component w/wo Presence of Germinal Centers or Eosinophils/Mast Cells w/wo Bone Infiltration (Osteolysis) | Macrophage infiltrate (grade ≥ 1) and lymphocytic (grade ≥ 2) w/wo Soft Tissue/Bone Necrosis |
| 4. Granulomatous w/wo Bone Infiltration (Osteolysis) | Any pattern with predominant presence of sarcoid-like granulomas |
| 5. [Lymphocytic]* | Interstitial and/or perivascular lymphocytic infiltrate without evidence of macrophage infiltrate |

*Observed only in one report [ref. 10].

A pure lymphocytic response without presence of any macrophage has been found only in one report [10] and most probably resulted from tissue sampling bias. A recent study on MoM THA and HRA of a single manufacturer[6] has confirmed the identification of macrophage predominant and lymphocytic predominant patterns with a variable degree of soft tissue necrosis, although the method of collection and examination of the tissue specimens is sub-optimal in several aspects: (a) one or even two specimen sample is insufficient for the identification of the cell type present and especially in cases with extensive soft tissue necrosis; (b) it is unclear the significance of pseudotumor (neo-synovium) and/or pseudocapsule sampling because most often they are in continuity and without any detectable cleavage plane at surgery; (c) bursal specimens can provide significant information only when they are removed intact and histological sections are taken from the bottom of the sac where the particulate wear debris usually accumulates; (d) histological sections cut at 10 μ instead of the customary 4-5 μ are too thick to provide fine cellular details. Moreover, the reactions cannot be classified as abrasion-induced by histological analysis and this is demonstrated in figure 3 which shows macrophage infiltrate and interstitial, large microplate-like particles present in MoM LHTHA implants, generated predominantly by mechanically assisted crevice/fretting corrosion at the MAS/neck junction. The histopathological classification of ALTR/ARMD has identified groups of patients with a consistent pattern of response with variable intensity to similar metallic wear debris, indicative of the presence of a distinct immunological profile for each group, in sharp contrast with the suggestion that the response to metallic debris is individual, as reported in a study on the pathogenesis of ARMD based on different wear rates with similar histological response in cases of bilateral hip implants [11].

Several parameters of possible difficulty in the interpretation of the classifications/histological descriptions of ALTR/ARMD have been identified and can contribute to inter-observer variability: (a) distinction among surface layer of necrotic cell debris, superficial tissue necrosis, and acellular/paucicellular desmoplastic layer; (b) definition of granulomatous reaction; (c) grading of lymphocytic infiltrate; (d) grading of macrophage infiltrate; (e) vascular changes and aseptic lymphocytic-dominated vasculitis-associated lesion (ALVAL). They are shown in Fig. 1-6.

Surface Tissue Necrosis and Granulomatous Reaction

Classification of the necrosis of the neo-synovium and pseudocapsular soft tissue was originally reported in 2005 [12] and adopted with minor modifications in the following years [2,3]. They are reported in Table 2.

Table 2 Synovial membrane/tissue necrosis.
Davies (2005)

| | Synovial membrane |
|----------------|---|
| Layer 1 | surface membrane |
| Layer 2 | subsurface layer lying superficial to vascular structures |
| Layer 3 | vascular layer of the neocapsule |
| Layer 4 | tissues deep to the neocapsule, including fibrous tissue, fat, and muscle |

Campbell (2011)

| | Synovial lining | Tissue organization |
|----------|---|--|
| 0 | Intact | Normal |
| 1 | Focal loss of synovial surface, fibrin attachment may occur | Mostly normal tissue arrangement, small areas of synovial hyperplasia, focal necrosis may occur |
| 2 | Moderate to marked loss of synovial surface, fibrin attachment | Marked loss of normal arrangement, appearance of distinct cellular and acellular zones, thick fibrous layers may occur |
| 3 | Complete loss of synovium, abundant attached fibrin and /or necrosis of lining tissue | Perivascular lymphocytic aggregates mostly located distally, thick acellular areas may occur |

Natu (2012)

| | Synovial surface | Tissue necrosis |
|---------------------|---|---|
| Type/Grade 1 | Intact synovial surface epithelium | Type 2 surface |
| Type/Grade 2 | Loss of the synoviocyte layer without fibrin deposition | Either less than 25% of the tissue showed Type 4 necrosis or Type 3 surface |
| Type/Grade 3 | Loss of the synoviocyte layer with fibrin deposition | Between 25% and 75% showed Type 4 necrosis |
| Type/Grade 4 | Extensive necrosis with loss of architecture | >75% of the tissue sample showed Type 4 necrosis |

One added feature is the presence of fibrin exudate/attachment at the surface which in the large majority of the cases represents a layer of exfoliated necrotic macrophages of variable thickness as previously described [4, 13).

Surface tissue necrosis and various types of granulomatous reaction are presented in [Fig. 1](#). The eosinophilic layer of cell necrosis ([Fig. 1a](#)) observed in a hip bursa (upper-left inset) with presence of corrosion metallic microplates (lower-right inset, black arrows) can be differentiated from the superficial layer of soft tissue necrosis at low magnification ([Fig. 1b](#), upper tissue section) and at higher magnification (Fig. 8c) because the latter under polarized light shows presence of birefringent fascicles of collagen fibers (lower-right inset); superficial soft tissue necrosis needs also to be distinguished from the band of collagenous, desmoplastic reaction which can occur in neo-synovial membranes of similar macroscopic appearance and thickness ([Fig. 1b](#), lower tissue section) and shown in detail in [Fig. 1d](#), with a surface layer of variable thickness with numerous particle laden macrophages and a variable degree of cell necrosis. Tissue necrosis of high grade (grade 3 or grade 4) does not present any difficulty of recognition as shown in Fig. 7 a-d of this review article.

The definition of granulomatous reaction has also varied in reports of old and even recent literature by clinicians and pathologists, including also sheets of particle laden macrophages with presence of

multinucleated giant cells in cases of osteolysis [14-16]. This type of reaction has also been included in the group of foreign body reactions (FRB), which usually apply to a multinucleated giant cell reaction to foreign particles, which can engulf or surround large particulate material without digestion (frustrated phagocytosis). However, since it is a distinctive type observed in a small subset of patients with ALTR/ARMD [4] which has also been reported in a case of PE debris in a TKA implant with regional lymph node involvement [17] and in a case of massive metallic wear debris in a THA implant with lung involvement [18], it should be restricted to the occurrence of sarcoid-like epithelioid cell granulomas with giant cells containing or surrounding particulate material without (Fig. 1e), or with presence of an incomplete/complete lymphocytic or lymphoplasmacytic cuffing (Fig. 1f); they should also be distinguished from palisading macrophage reaction with central fibrinoid necrosis typical of a rheumatoid nodule or granuloma annulare (Fig. 1g) and necrotizing granulomas with giant cells, indicative of Mycobacterium species or fungal infection (Fig. 8h). This distinction is important to avoid possible misdiagnosis of ALTR/ARMD in MoM and non-MoM implants in presence of lymphoplasmacytic infiltrate and granulomas as recently reported in a non-MoM THA case [19].

In summary, it is highlighted the criteria used for the distinction of a surface layer of cell death/necrosis from superficial tissue necrosis and desmoplastic fibrosis and the definition of granulomatous reaction reserved to the presence of sarcoid-like granulomas and not of sheets of macrophages with foreign body multinucleated giant cells.

Lymphocytic infiltrate grading

The perivascular/interstitial lymphocytic infiltrate in the periprosthetic soft tissue has been generally classified with a semiquantitative scale and the proposed classifications [2,3, 12, 13, 20, 21] are shown in Table 3.

Table 3 Histological classification of lymphocytic infiltrate in ALTR/ARMD

| Davies (2005) | | | |
|-----------------------|--|---------------------------|--|
| | Diffuse (Interstitial) 400x | Perivascular 4x400 | |
| 0 None | <10 | 0 | |
| + Few | 11-30 | 1-2 | |
| ++ Many | 31-50 | 3-6 | |
| +++ Abundant | 51-100 | 7-10 | |
| ++++ Excessive | >100 | >10 | |

| Fujishiru (2011) | | | |
|-------------------------|--|----------------------------------|------------------------------|
| | General lymphocytes or plasma cells (diffuse) | Perivascular | |
| | | Layers of lymphocytes | Number of vessels |
| 0 | <10 cells/HPF | 0 | 0 |
| + | 11-30 cells/HPF | 1 to 3 layers/HPF | 1 to 2 |
| ++ | 31-50 cells/HPF | 4 to 10 layers/HPF | 3 to 6 |
| +++ | 51-100 cells/HPF | >10 layers/HPF | 7 to 10 |
| ++++ | >100 cells/HPF | | >10 |

Natu (2012)

| Lymphocyte cuff thickness | |
|----------------------------------|-------------|
| Absent | |
| + | <0.25 mm |
| ++ | 0.25-0.5 mm |
| +++ | 0.5-0.75 mm |
| ++++ | >0.75 mm |

| Campbell (2012) | |
|-------------------------------|---|
| Lymphocytic infiltrate | |
| 0 | Minimal inflammatory cell infiltrates |
| 1 | Predominantly macrophages, occasional lymphocytes may occur |
| 2 | Mix of macrophages and lymphocytes, either diffuse and/or small (<50% HPF) perivascular aggregates |
| 3 | Predominantly lymphocytes, mostly in multiple, large (>50% HPF) perivascular aggregates, follicles may be present |

| Grammatopoulos (2013) | |
|--|---------------------|
| Perivascular lymphocytic infiltrate | |
| 0 | No evidence |
| 1 | < 5 cells thick |
| 2 | 5 to 10 cells thick |
| 3 | >10 cells thick |

| Langton (2018) | |
|-----------------------|------------------------------|
| Vascular cuff | |
| 0 | None |
| 1 | Small perivascular |
| 2 | Large perivascular |
| 3 | Large confluent perivascular |

A similar classification has not been reported for the bone marrow, although lymphocytic aggregates have been described [1, 4, 22]. Examples of the grading of the perivascular lymphocytic infiltrate are provided in App. III [Fig. 2a, b, d, f](#) for soft tissue and App. III [Fig. 2c, e, g](#) for the bone marrow, using the grading method proposed by Natsu et al [3] and for the interstitial lymphocytic infiltrate in [Fig. 2h](#). Grade 1 for soft tissue is shown in [Fig. 2a](#) associated with particle laden macrophages; it is not shown for bone specimens because we have not found cases without areas of higher grade. Grade 2 for the soft tissue ([Fig. 2b1 and 2b2](#)) shows the difference between a lymphocytic infiltrate (b1) and a mixed lymphocytic and plasmacytic infiltrate (b2) and in the bone marrow associated with particle-laden macrophages indicated by black arrow ([Fig. 2c](#)) and soft tissue lymphocytic infiltrate shown in inset. Grade 3 in soft tissue is most often seen as confluent smaller aggregates with involvement of several capillaries ([Fig. 2d](#)) and/or with the formation of small reactive germinal centers which can also be observed in the bone

marrow (Fig. 2e). Grade 4 is usually associated with reactive germinal centers in soft tissue and bone marrow which can be large both in the soft tissue (Fig. 2f) and in the bone marrow (Fig. 2g), in this case also with evident mitotic activity (black arrows). The interstitial lymphocytic infiltrate (Fig. 2h) is more difficult to assess especially in the crowded cellular setting of ALTR/ARMD, unless the lymphocytes are identified by immunohistochemistry as shown in the two insets stained for B cells (CD20) and T cells (CD3).

The count of the rows of lymphocytes around the venules cannot be accurate and leads to interobserver variability for several reasons: (a) the lymphocytic infiltrate is frequently eccentric to the venule location (Fig. 9b1) or confluent with several venules involved (Fig. 2d); (b) lymphocyte rows are not easily identifiable when admixed with plasma cells (Fig. 2b2); (c) lymphocyte rows cannot be measured in the presence of germinal centers (Fig. 2e, f, g). Therefore, the semi-quantitative analysis of the lymphocytic infiltrate should be performed for the perivascular and also the bone marrow aggregates measuring the average lymphocytic cuff/aggregate thickness as previously reported [3] whereas the interstitial component can be evaluated with a reproducible degree of accuracy only by a quantitative analysis at high power ($\times 400$), expressed as percentage of positive cells per mm^2 after immunohistochemical staining for a B-cell (CD20) and T-cell (CD3) markers.

Grade 1 reactive lymphocytic aggregates in the soft tissue and in the bone marrow can be observed in specimens of hip and other joints replacements for mechanical osteoarthritis and should be considered non-specific for ALTR/ARMD, unless numerous (≥ 5 in soft tissue and bone histological sections) and consistently associated with particle laden macrophages. An increase of T cell lymphocytes in the bone marrow associated with ageing has also been reported [23]. Grade 2 to grade 4 infiltrates also with formation of germinal centers can be observed especially in large bone specimens and almost invariably exhibit corresponding lymphocytic infiltrate in the periprosthetic soft tissue and are associated to particle laden macrophages, indicating that the macrophage infiltrate is necessary to modulate the lymphocytic infiltrate in different subsets of patients. The number of total perivascular lymphocytic infiltrates is suggested as an adjuvant criterion for the evaluation of grade 1 and in cases of different grades where the higher value should be present in at least 3 aggregates. In exceptional cases, step sections of the tissue block might be performed to capture the real size of the aggregates. The diagnosis of a treated or untreated rheumatoid disorder should always be noted in a comment to the case in the pathological report because in these cases a similar, a florid perivascular and interstitial lymphoplasmacytic infiltrate can also be observed at the time of implantation (time zero).

If multiple tissue sections are submitted for histological examination, the number of cases of uncertain classification can be effectively reduced to a minimum with very limited intraobserver and interobserver variability. The semi-quantitative histological classifications of the lymphocytic infiltrate based only on routine H&E staining are to a large extent insufficient for the identification of the sub-type(s) of immunoreaction which occur in response to the wear particles and more-in-depth analysis of the various classes of lymphocytes and other inflammatory cells involved needs to be performed on the periprosthetic tissue collected fresh at surgery [24], in a fashion which could be similar to studies performed in patients affected by rheumatic inflammatory disorders [25, 26]. The results of these analyses could be more informative than the *in vitro* and murine model studies on metal sensitization using particles composed of a single metal and of a standard size, an oversimplification of the physical and chemical properties of corrosion metallic particles released by orthopedic implants in patients and based on the assumption that the reaction is predominantly due to CD4^+ Th1 lymphocytes [27]. The results of these studies, although useful to elucidate possible pathways of inflammation, should be

taken with caution especially when therapeutic strategies are proposed to prevent or mitigate ALTR/ARMD.

The term delayed hypersensitivity type IV reaction (DTH) was implemented to describe a T-cell reaction to tuberculin and has become a generic term encompassing all T-cell mediated reactions even if different cytokines can be produced leading to distinct clinical disease [28]. This type of immunologically mediated reaction ascribed to corrosion metallic particles/metallic ions [29-34] needs to be refined according to the histopathological analysis of the periprosthetic soft tissue, taking into consideration T-cell rich lymphocytic infiltrates in the bone marrow, associated to particle laden macrophages. In particular, four distinct sub-types of DTH to drugs usually occurring in skin for drug hypersensitivity reactions have been reviewed [28]. The occurrence of three of the four subtypes in the periprosthetic tissue is supported by the histopathological examination of the periprosthetic tissue: type IVa, mediated by Th1 lymphocytes (IFN- γ) with monocyte activation and granuloma formation; type IVb, mediated by Th2 lymphocytes (IL-5 and IL-4) with eosinophilic and mast cell inflammation; and type IVc, mediated by cytotoxic lymphocytes (perforin and granzyme B), CD8⁺ mediated cell death. The three subtypes of DTH can explain some of the radiological and histological findings and the quantitative and qualitative differences in the prevalence of ALTR/ARMD in MoM HRA, MoM THA, and non-MoM CoCr DMNTHA and TMZF stem, as shown in a study of nanoanalysis of metallic particles and correlation with periprosthetic soft tissue and bone inflammatory infiltrate from the three configurations [28]. In particular, the model of non-MoM THA with CoCrDMN and TMZF stem with a high number of ALTR/ARMD represents an interesting case study for the subtypes of DTH because has expressed a high level of IFN- γ and IL-6 consistent with a Th1 mediated reaction [33] with a small subset of patients with predominant sarcoid-like granulomatous response, but also a high number of cases with eosinophils and mast cells at histological examination [4], consistent with a Th2 mediated component and therefore suggestive of a mixed type IVa and type IVb response, corroborated by the presence of a mixed T-cell population positive for T-bet (Th1) and GATA-3 (Th2) by immunohistochemistry [5]. Moreover, the group of patients exhibiting skeletal muscle involvement (Fig. 9f) could express a type IVc reaction through cytotoxic lymphocytes CD8⁺/CD4⁺ as described in cases of polymyositis [35]. In addition, the complexity of the interrelation between lymphocytes, macrophages, endothelial cells, and stromal fibroblasts is exemplified by the role and regulation of the vascular endothelial growth factor (VEGF) and its receptors 1 and 2 in the occurrence of aseptic loosening of THA [36]. In this study, vascular endothelial growth factor 1 (VEGFR1) and 2 (VEGFR2) were not up-regulated by hypoxia, but VEGFR1 mRNA was increased by 23 folds by IL-4, which can derive from mast cells but also by Th2 lymphocytes. Consequently, in cases of ALTR/ARMD characterized by a predominant Th2 population of T lymphocytes and a high number of mast cells, osteolysis might occur at a higher rate and after a shorter implantation time than the one for other groups. Although ALTR/ARMD has been attributed in large part to a T cell infiltrate, in a distinct subset of patients with MoM implants, a prominent component of B lymphocytes with the formation of tertiary lymphoid organs (germinal centers) also occurs [37]. At last, the role of dendritic cells in the host response to implant wear debris and their interaction with adaptive immune cells [38, 39] should also be considered in the development of ALTR/ARMD.

Macrophage infiltrate grading

A semiquantitative grading of the macrophage infiltrate in the periprosthetic soft tissue has been reported by a few investigators for MoM HRA and THA and CoC THA [3, 13, 40] and it is summarized in [Table 4](#).

Table 4 Macrophage infiltrate classification in periprosthetic soft tissue

| Natu (2012) | |
|--------------------------|------------------|
| Macrophage sheets | Thickness |
| 0 | Absent |
| 1 | <1 mm |
| 2 | 1≥2 mm |
| 3 | >2 mm |

| Grammatopoulos (2013) | |
|------------------------------|----------------------------------|
| Macrophages | Semi-quantitative grading |
| 0 | Absent |
| 1 | Few |
| 2 | Many |
| 3 | Abundant |
| 4 | |

| Esposito (2013) | |
|------------------------|---------------------------------|
| Macrophages | Infiltrate grading |
| 0 | Low cellularity, no macrophages |
| 1 | Mild (<2/HPF) |
| 2 | Moderate (2 to 49/HPF) |
| 3 | Marked (≥50/HPF) |

Examples of grading of the macrophage infiltrate for soft tissue and bone marrow are shown in App. III [Fig. 3](#) through App. III [Fig. 5](#). Grade 1 in neo-synovial membrane in a case of MoM HRA with implantation time of 5 months shows well-preserved neo-synovium ([Fig. 3a](#)) and the inflammatory infiltrate composed of scattered macrophages containing tribocorrosion metallic particles, lymphocytes, and eosinophils ([Fig. 3b](#)). Grade 1 macrophage infiltrate in bone, in a case of MoM LHTHA with CoCr MAS, is admixed to mature and immature hematopoietic marrow cells ([Fig. 3c](#)), more evident at higher magnification ([Fig. 3d](#), black arrows). Grade 2 in the neo-synovium in a case of non-MoM THA with CoCr DMN and TMZF stem shows a surface macrophage infiltrate ([Fig. 4a](#)) containing aggregates/agglomerates of greenish corrosion particles generated at the neck-stem interface at higher magnification ([Fig. 4b](#), black arrow) and presence of transmural tissue necrosis with deep lymphocytic infiltrate in another area shown in inset; another example is shown in a case of MoM LHTHA with CoCr MAS with macrophage infiltrate < 2 mm thick ([Fig. 4c](#)) with cell details ([Fig. 4d](#)) and evident intracellular content of metallic particle content in a semithin section shown in inset. Grade 3 in the neo-synovium and grade 2 and 3 in the bone marrow are shown in App. III [Fig. 5](#). In a case of MoM HRA, grade 3 in the soft tissue with macrophage layer >2 mm is shown in papillary configuration and corresponding tissue section ([Fig. 5a](#)) with details of the macrophage infiltrate ([Fig. 5b](#)) and grade 2 bone involvement is shown in the femoral head ([Fig. 5a](#)) and corresponding tissue section with partial marrow effacement ([Fig. 5c](#)). Another case of grade 2 bone involvement in a case of MoM HRA ([Fig. 5d](#) and [5e](#)) shows a mechanism of implant loosening: normal metallic stem/bone interface fibrous membrane ([Fig. 5d](#), black arrows) is observed in the distal portion of the femoral head (inset) and macrophage infiltrate in the bone marrow lifting the stem/bone interface fibrous membrane by interposition in [Fig. 5e](#) with detail in inset, leading to loosening of the component. Grade 3 soft tissue and bone involvement, in a case of MoM HRA shows thickness of >2 mm (black bar) and involvement of approximately 50% of the femoral

head (Fig. 5f) with detail of the soft tissue macrophage infiltrate (Fig. 5g) and particle content shown in a semithin section (inset) and of complete effacement of the bone marrow (Fig. 5h).

Grading systems for macrophage infiltrate have been reported only for the soft tissue and not for the bone infiltrate, although its presence has been documented [1, 4]. These grading systems can have high intra-observer and inter-observer variability especially for the intermediate grade for the following reasons: (a) cutoff point between grade 2 and grade 3 cannot be accurately measured and is subjective by its definition (thickness of 2 mm, 49 macrophages/HPF; many versus abundant macrophages); (b) the amount of soft tissue and/or bone necrosis can affect significantly the total count. Grade 1 is an infrequent occurrence in the periprosthetic soft tissue of MoM and non-MoM cases of ALTR/ARMD and observed only after a very short implantation time as shown in Fig. 3a and 3b. It can be observed more frequently in the periprosthetic bone (Fig. 3c and d) because it occurs usually at a later implantation time which would be closer to the time of histological observation at implant revision time. Moreover, the biological significance of the quantification of the macrophage infiltrate in the soft tissue is uncertain while in the bone could be an indicator of the probability of implant loosening. The thickness of the surface layer of the exfoliated forms can be used as an index of the cell toxicity of the metallic ions/particles. It is reasonable to assume that the cohorts MoM HRA and MoM THA configurations over ten years of implantation time will exhibit grade 2 or grade 3 of macrophage infiltrate in the periprosthetic soft tissue of almost all the revised cases.

The occurrence of macrophage infiltration in the bone marrow can be underestimated if specimens of curetted osteolytic cavities, frequently described at surgery as “cheesy material” are not sent for histological examination. In need of long-term studies is the relationship between particle laden macrophages with hematopoietic marrow mature and immature cells [41], as found also in distant locations from the implanted hip and knee joint in a post-mortem study [42]. This is particularly important for the patients affected by autoimmune diseases and under biologic disease-modifying treatments. Moreover, the mechanism(s) of osteolysis, previously attributed to orthopedic cement and/or polyethylene debris originated from non-MoM total joint arthroplasty implants and also identified in a relevant number of cases with MoM bearing surface as previously described [43] should be re-assessed in search of a possible common mechanism. Up to the present time, the central role of the macrophage in periprosthetic osteolysis has been established [44], although attributed to uptake and phagocytosis of wear particles by tissue resident macrophages with expression of various cytokines and chemokines inducing the expression of the receptor activator of nuclear factor-kappa-beta (RANK) ligand (RANKL) for osteoclastic stimulation and bone resorption [44, 45]. In particular, interferon γ (IFN- γ) stimulates osteoclast formation and bone loss via T cell activation in murine models [46] and the very high levels occurring in ALTR/ARMD [33] could significantly contribute to the extent of osteolysis, especially in the cases with T cell infiltrate in the bone marrow.

One of the most used experimental models used to simulate periprosthetic osteolysis is the murine calvarium mainly because it is simple and elicits a short-term reaction. However, this model is based on the concept that osteolysis is the end result of osteoclastic resorption with formation of empty bone defects. This is a misrepresentation of the reaction in the clinical setting where the spaces are filled with a variable amount of particle laden macrophages with or without increased osteoclastic activity as shown in App. III Fig. 3d and Fig. 5c, 5e and 5h. Murine models taking into account the chronicity and usually slow progression of the reaction have been proposed, although with use of wear particles produced by simulators instead of retrieved implants and directly injected into the animal bone instead of the joint space where they are generated *in vivo* [47]. The hypothesis that wear-particle induced oxidative stress of the macrophages initiates the cascade of reactions leading to osteolysis after metal-

on-polyethylene (MoP) THA has been analyzed in one *in vivo* study, finding a connection between oxidative stress and development of osteolysis [48]. This line of research may be promising because clinically significant macrophage invasion of the bone marrow occurs more frequently when wear particles with a high degree of oxidation are generated, such as polyethylene and mixed corrosion and conventional metallic particles. This observation is corroborated by reduced osteolytic activity by anti-oxidation treatment of UHMW PE particles [49] and clinical studies showing absence/low prevalence of osteolysis and implant loosening in MoP THA with highly cross-linked polyethylene [50]. In support, studies on a ceramic-on-ceramic (CoC) THA have also reported very low rate of aseptic loosening and clinical studies very low prevalence of osteolysis/implant loosening in ceramic-on-ceramic (CoC) THA [51, 52], although high prevalence (22%) has been observed in one study on alumina-ceramic CoC THA [53], which might have been caused by factors different from macrophage reaction to wear debris [54].

The explanation for the massive influx of macrophages from the neo-synovium migrating into the periprosthetic bone and formation of masses with significant bone resorption is still unresolved and might be better understood by studying the activation of macrophage motility in the extracellular matrix by amoeboid and/or mesenchymal fashion [55] and chemotactic factors produced by marrow cells as well as factors produced by macrophages in the bone environment leading to increased osteoclastic differentiation and activity, such as the recently described netrin-1 [56]. The examination *in vitro* of the macrophages exposed to wear particles generated *in vivo* under different spatial constraints and extracellular matrix stiffness also provides valuable data on how the macrophages are activated into a spectrum of states, from pro-inflammatory (M1) to pro-healing (M2) phenotypes [57]. Recently, the study of the presence of implant metallic wear debris in the intertrabecular and trabecular bone highlights the importance of the macrophage infiltrate in the bone marrow for possible long-term effects of biomaterial/host interaction [58].

Fibroblast proliferation and activity

The role of intimal and subintimal fibroblasts in ALTR/ARMD is difficult to assess by histological examination because of the small size of the fibroblasts embedded in abundant collagenous matrix in the flat neo-synovial membrane and in the papillary/polypoid fibrovascular proliferation with predominant macrophage infiltrate. Recent research has demonstrated activity *in vitro* when exposed to metallic nanoparticles which are consistent with their enhanced production of collagen *in vivo* [59]. More research should be performed on the relationship between macrophages and fibroblasts and especially on the effects of the mechanical properties of the collagenous matrix for the macrophage production of inflammatory cytokines.

Vascular changes and aseptic lymphocytic-dominated vasculitis-associated lesion (ALVAL)

Several vascular changes have been described occurring in ALTR [3, 4, 37]. They are presented in App. III [Fig. 6a](#) through [6d](#). The most consistent is the presence of high endothelial venules with migrating lymphocytes ([Fig. 6a](#)) with detail of the venule in inset. Occlusion of the capillary/venule lumen ([Fig. 6b](#)), capillary/venule onion skin pattern ([Fig. 6c](#)), and capillary/venule concentric or eccentric wall thickening ([Fig. 6d](#)) can also be observed, although non-specific of ALTR/ARMD. Necrosis of the vascular wall with or without inflammatory infiltrate was not detected in any of the cases examined, unless in areas of transmural soft tissue necrosis. The relationship between particle laden macrophages and particle wear and the development of high endothelial venules with subsequent lymphocyte migration and trafficking should be studied in depth to better understand quantitative and qualitative aspects of the host response to the corrosion metallic wear particles, beyond the stimulation of endothelial cells by metallic ions [60] or the effect of Co and Cr ions on lymphocytic migration [61].

Until the introduction of the second generation of MoM implants the main ALTR has been the occurrence of osteolysis, dependent on the amount, size, composition, and oxidative state of particles of implant wear debris and in particular orthopedic cement and polyethylene with or without metallic debris mainly generated by surface abrasion/adhesion/erosion. The lymphocytic reaction occurring in MoM HRA and THA was first reported in 2005 [12] and later defined under the acronym of ALVAL. Although even in the original report there was a significant quantitative variability of the lymphocytic infiltrate in the cases described, the acronym ALVAL became a popular term encompassing a full spectrum of a reaction with different clinical outcomes on the assumption that all the cases could progress to a lymphocytic response associated to soft tissue/bone necrosis with or without skeletal muscle and tendon involvement. The acronyms ALTR and ARMD were subsequently proposed to acknowledge the spectrum of the adverse reaction as an umbrella term to describe for the former macrophage and lymphocytic reactions and for the latter joint failures associated with pain, a large sterile effusion of the hip and/or macroscopic necrosis/metallosis [62, 63]. Although both terms have been originally intended for local tissue reactions and have been used in this manuscript as equivalent, a possible difference between the two terms is that where ALTR specifies local, ARMD may also be used for systemic effects. The term ALVAL is still used at the present time for the lymphocytic reaction and especially with soft tissue necrosis even if it is widely acknowledged that the infiltrate is actually perivascular and/or band-like/interstitial without any damage of the vascular wall, distinctive of vasculitis. Our review confirms the presence of high endothelial venules as the most frequent finding in the adverse reactions associated with a lymphocyte-rich infiltrate and also the observation of other non-specific reactive changes in absence of the findings of a bona fide vasculitis, as defined by the Chapel Hill consensus classification [64].

In summary, we propose that the term ALVAL should be substituted with the retention of the two acronyms ALTR and ARMD, modified as adverse local predominantly lymphocytic reaction (ALLTR) and/or adverse predominantly lymphocytic reaction to metal debris (ALRMD) and adverse local predominantly macrophage reaction (ALMTR) and/or adverse predominantly macrophage reaction to metal debris (AMRMD). Because of the possible reference to either local or systemic effects for ARMD, local may be added resulting in ALLRMD and AMLRMD, respectively.

References

1. **Mahendra G, Pandit H, Kliskey K, Murray D, Gill HS, Athanasou N.** Necrotic and inflammatory changes in metal-on-metal resurfacing hip arthroplasties. Relation to implant failure and pseudotumor formation. *Acta Orthopaedica* 2009;80: 653-59.
2. **Campbell P, Ebrahimzadeh E, Nelson S, Takamura K, De Smet K, Amstutz HC.** Histological features of pseudotumor-like tissues from metal-on-metal hips. *Clin Orthop Relat Res* 2010;468:2321-27.
3. **Natu S, Sidaginamale RP, Gandhi J, Langton DJ, Nargol AV.** Adverse reactions to metal debris: histopathological features of periprosthetic soft tissue reactions seen in association with failed metal on metal hip arthroplasties. *J Clin Pathol* 2012;65:409-18.
4. **Ricciardi B, Nocon AA, Jerabek SA, Wilner G, Kaplowitz E, Goldring SR, et al.** Histopathological characterization of corrosion product associated adverse local tissue reaction in hip implants: a study of 285 cases. *BMC Clin Pathol* 2016;16:3. doi: 10.1186/s12907-016-0025-9.
5. **Perino G, Ricciardi BF, Jerabek SA, Martignoni G, Wilner G, Maass D, et al.** Implant based differences in adverse local tissue reaction in failed total hip arthroplasties: a morphological and immunohistochemical study. *BMC Clin Pathol* 2014;14:39. doi: 10.1186/1472-6890-14-39.

6. **Reito A, Lehtovirta L, Parkkinen J, Eskelinen A.** Histopathological patterns seen around failed metal-on-metal hip replacements: Cluster and latent class analysis of patterns of failure. *J Biomed Mater Res* 2019;1–12. doi: 10.1002/jbm.b.34460.
7. **Nawabi DH, Gold S, Lyman S, Fields K, Padgett DE, Potter HG.** MRI predicts ALVAL and tissue damage in metal-on-metal hip arthroplasty. *Clin Orthop Relat Res.* 2014;472:471-81.
8. **Smeekes C, Cleven AHG, van der Wal BCH, Dubois SV, Rouse RW, Ongkiehong BF, et al.** Current pathologic scoring systems for metal-on-metal THA revisions are not reproducible. *Clin Orthop Relat Res* 2017;475:3005-11.
9. **Bauer TW.** CORR Insights: Current pathologic scoring systems for metal-on-metal THA revisions are not reproducible. *Clin Orthop Relat Res* 2017;475:3012-14.
10. **Berstock JR, Baker RP, Bannister GC, Case CP.** Histology of failed metal-on-metal hip arthroplasty; three distinct sub-types. *Hip Int* 2014;24:243–8.
11. **Lehtovirta L, Reito A, Lainiala O, Parkkinen J, Hothi H, Henckel J, et al.** Host-specific factors affect the pathogenesis of adverse reaction to metal debris. *BMC Musculoskelet Disord* 2019;20:195. doi: 10.1186/s12891-019-2578-0.
12. **Davies AP, Willert HG, Campbell PA, Learmonth ID, Case CP.** An unusual lymphocytic perivascular infiltration in tissues around contemporary metal-on-metal joint replacements. *J Bone Joint Surg Am* 2005;87:18–27.
13. **Grammatopoulos G, Pandit H, Kamali A, Maggiani F, Glyn-Jones S, Gill HS, et al.** The correlation of wear with histological features after failed hip resurfacing arthroplasty. *J Bone Joint Surg Am* 2013;95:e81 (1-10).
14. **Griffiths HJ, Burke J, Bonfiglio TA.** Granulomatous pseudotumors in total joint replacement. *Skeletal Radiol.* 1987;16:146-52.
15. **Santavirta S, Konttinen YT, Bergroth V, Eskola A, Tallroth K, Lindholm TS.** Aggressive granulomatous lesions associated with hip arthroplasty. Immunopathological studies. *J Bone Joint Surg Am* 1990;72:252-58.
16. **Slullitel PAI, Brandariz R, Oñativia JI, Farfalli G, Comba F, Piccaluga F, Buttaro M.** Aggressive granulomatosis of the hip: a forgotten mode of aseptic failure. *Int Orthop* 2019;43:1321-328.
17. **Jacobs JJ, Urban RM, Wall J, Black J, Reid JD, Veneman L.** Unusual foreign-body reaction to a failed total knee replacement: simulation of a sarcoma clinically and a sarcoid histologically. A case report. *J Bone Joint Surg Am* 1995;77:444-51.
18. **Balbouzis T, Georgiadis T, Grigoris P.** Granulomatous lung disease: a novel complication following metallosis from hip arthroplasty. *Hip Pelvis* 2016;28:249-53.
19. **Jandl NM, Rolvien T, Gätjen D, Jonitz-Heincke A, Springer A, Krenn V, et al.** Recurrent arthrocele and sterile sinus tract formation due to ceramic wear as a differential diagnosis of periprosthetic joint infection—a case report. *Acta Orthop* 2019;16:1-6.
20. **Grammatopoulos G, Munemoto M, Pollalis A, Athanasou NA.** Correlation of serum metal ion levels with pathological changes of ARMD in failed metal-on-metal-hip-resurfacing arthroplasties. *Arch Orthop Trauma Surg* 2017;137:1129-37.
21. **Fujishiro T, Moojen DJ, Kobayashi N, Dhert WJ, Bauer TW.** Perivascular and diffuse lymphocytic inflammation are not specific for failed metal-on-metal hip implants. *Clin Orthop Relat Res* 2011;469:1127-133.
22. **Zustin J, Amling M, Krause M, Breer S, Hahn M, Morlock MM, et al.** Intraosseous lymphocytic infiltrates after hip resurfacing arthroplasty: a histopathological study on 181 retrieved femoral remnants. *Virchows Arch* 2009;454:581-88.
23. **Naismith E, Pangrazzi L, Grasse M, Keller M, Miggitsch C, Weinberger B, et al.** Peripheral antibody concentrations are associated with highly differentiated T cells and inflammatory

processes in the human bone marrow. *Immun Ageing* 2019;16:21. doi: 10.1186/s12979-019-0161-z. eCollection 2019.

24. **Krenn, V and Perino, G.** Histological diagnosis of implant-associated pathologies., Berlin Heidelberg: Springer-Verlag, 2017.
25. **Donlin LT, Rao DA, Wei K, Slowikowski K, McGeachy MJ, Turner JD, et al.** Methods for high-dimensional analysis of cells dissociated from cryopreserved synovial tissue. *Arthritis Res Ther* 2018;20:139. doi: 10.1186/s13075-018-1631-y.
26. **Stephenson W, Donlin LT, Butler A, Rozo C, Bracken B, Rashidfarrokhi A, et al.** Single-cell RNA-seq of rheumatoid arthritis synovial tissue using low-cost microfluidic instrumentation. *Nat Commun* 2018;23:791. doi: 10.1038/s41467-017-02659-x.
27. **Samelko L, Caicedo MS, Jacobs J, Hallab NJ.** Transition from metal-DTH resistance to susceptibility is facilitated by NLRP3 inflammasome signaling induced Th17 reactivity: Implications for orthopedic implants. *PLoS One* 2019;14:e0210336. doi: 10.1371/journal.pone.0210336. eCollection 2019.
28. **Pichler VJ.** Delayed drug hypersensitivity reactions. *Ann Intern Med* 2003; 139:683-93.
29. **Hallab N, Merritt K, Jacobs JJ.** Metal sensitivity in patients with orthopaedic implants. *J Bone Joint Surg Am* 2001;83:428-36.
30. **Pandit H, Vlychou M, Whitwell D, Crook D, Luqmani R, Ostlere S, et al.** Necrotic granulomatous pseudotumours in bilateral resurfacing hip arthroplasties: evidence for a type IV immune response. *Virchows Arch* 2008;453:529-34.
31. **Thyssen JP, Johansen JD, Menné T, Lidén C, Bruze M, White IR.** Hypersensitivity reactions from metallic implants: a future challenge that needs to be addressed. *Br J Dermatol* 2010;162:235-36.
32. **Pinson ML, Coop CA, Webb CN.** Metal hypersensitivity in total joint arthroplasty. *Ann Allergy Asthma Immunol* 2014;113:131-36.
33. **Furrer S, Scherer Hofmeier K, Grize L, Bircher AJ.** Metal hypersensitivity in patients with orthopaedic implant complications-A retrospective clinical study. *Contact Dermatitis* 2018;Jun 11. doi: 10.1111/cod.13032.
34. **Caicedo MS, Solver E, Coleman L, Jacobs JJ, Hallab NJ.** Females with unexplained joint pain following total joint arthroplasty exhibit a higher rate and severity of hypersensitivity to implant metals compared with males: implications of sex-based bioreactivity differences. *J Bone Joint Surg Am* 2017;99:621-28.
35. **Pandya JM, Venalis P, Al-Khalili L, Shahadat Hossain M, Stache V, Lundberg IE, et al.** CD4+ and CD8+ CD28 (null) T cells are cytotoxic to autologous muscle cells in patients with polymyositis. *Arthritis Rheumatol* 2016;68:2016-26.
36. **Waris V, Sillat T, Waris E, Virkki L, Mandelin J, Takagi M, Konttin IT.** Role and regulation of VEGF and its receptors 1 and 2 in the aseptic loosening of total hip implants. *J Orthop Res* 2012;30:1830-36.
37. **Mittal S, Revell M, Barone F, Hardie DL, Matharu GS, Davenport AJ et al.** Lymphoid aggregates that resemble tertiary lymphoid organs define a specific pathological subset in metal-on-metal hip replacements. *PLoS One* 2013;8:e63470.
38. **Vasilijic S, Savic D, Vasilev S, Vucevic D, Gasic S, Majstorovic I, et al.** Dendritic cells acquire tolerogenic properties at the site of sterile granulomatous inflammation. *Cell Immunol* 2005;233:148-157.
39. **Keselowsky BG, Lewis JS.** Dendritic cells in the host response to implanted materials. *Semin Immunol* 2017;29:33-40.

40. **Esposito C, Maclean F, Campbell P, Walter WL, Walter WK, Bonar FS.** Periprosthetic tissues from third generation alumina-on-alumina total hip arthroplasties. *J Arthroplasty* 2013;28:860-66.
41. **Ort MJ, Geissler S, Rakow A, Schoon J.** The allergic bone marrow? the immuno-capacity of the human bone marrow in context of metal-associated hypersensitivity reactions. *Front Immunol* 2019;10:2232. doi: 10.3389/fimmu.2019.02232. eCollection 2019.
42. **Hall DJ, Pourzal R, Jacobs JJ, Urban RM.** Metal wear particles in hematopoietic marrow of the axial skeleton in patients with prior revision for mechanical failure of a hip or knee arthroplasty. *J Biomed Mater Res B Appl Biomater* 2019;107:1930-936.
43. **Huber, M., Reinisch, G., Zenz, P., Zweymüller, K., & Lintner, F. (2010).** Postmortem study of femoral osteolysis associated with metal-on-metal articulation in total hip replacement. *J Bone Joint Surg Am* 2010;92(8), 1720–1731. doi:10.2106/jbjs.i.00695
44. **Nich C, Takakubo Y, Pajarinen J, Gallo J, Konttinen YT, Takagi M, Goodman SB.** The role of macrophages in the biological reaction to wear debris from artificial joints. *J Long Term Eff Med Implants* 2016;26:303-09.
45. **Ollivere B, Wimhurst JA, Clark IM, Donell ST.** Current concepts in osteolysis. *J Bone Joint Surg Br* 2012;94:10-15.
46. **Gao Y, Grassi F, Ryan MR, Terauchi M, Page K, Yang X, et al.** IFN- γ stimulates osteoclast formation and bone loss in vivo via antigen-driven T cell activation. *J Clin Invest* 2007;117:122-32.
47. **Pajarinen J, Nabeshima A, Lin TH, Sato T, Gibon E, Jämsen E, et al.** Murine model of progressive orthopedic wear particle-induced chronic inflammation and osteolysis. *Tissue Eng Part C Methods* 2017;23:1003-11.
48. **Steinbeck M, Jablonowski MS, Parvizi J, Freeman TA.** The role of oxidative stress in aseptic loosening of total hip replacements. *J Arthroplasty* 2014;29:843–49.
49. **Green JM, Hallab NJ, Liao YS, Narayan V, Schwarz EM, Xie C.** Anti-oxidation treatment of ultra-high molecular weight polyethylene components to decrease periprosthetic osteolysis: evaluation of osteolytic and osteogenic properties of wear debris particles in a murine calvaria model. *Curr Rheumatol Rep* 2013;15:325. doi: 10.1007/s11926-013-0325-3.
50. **Rames RD, Stambough JB, Pashos GE, Maloney WJ, Martell JM, Clohisy JC.** Fifteen-year results of total hip arthroplasty with cobalt-chromium femoral heads on highly cross-linked polyethylene in patients 50 years and less. *J Arthroplasty* 2019;34:1143-49.
51. **Hu D, Tie K, Yang X, Tan Y, Alaidaros M, Chen L.** Comparison of ceramic-on-ceramic to metal-on-polyethylene bearing surfaces in total hip arthroplasty: a meta-analysis of randomized controlled trials. *J Orthop Surg Res.* 2015;10:22. doi: 10.1186/s13018-015-0163-2.
52. **Kim YH, Park JW, Kim JS.** Long-Term Results of Third-Generation Ceramic-on-Ceramic Bearing Cementless Total Hip Arthroplasty in Young Patients. *J Arthroplasty.* 2016;31:2520-24.
53. **Yoon TK, Rowe SM, Jung ST, Seon KJ.** Osteolysis in association with THA with ceramic bearing surfaces. *J Bone Joint Surg.* 1988;80A:1459-68.
54. **Savarino L, Baldini N, Ciapetti G, Pellacani A, and Giunti A.** Is wear debris responsible for failure in alumina-on-alumina implants? Clinical, histological, and laboratory investigations of 30 revision cases with a median follow-up time of 8 years. *Acta Orthop.* 2009;80:162-67.
55. **Van Goethem E, Poincloux R, Gauffre F, Maridonneau-Parini I, Le Cabec V.** Matrix architecture dictates three-dimensional migration modes of human macrophages: differential involvement of proteases and podosome-like structures. *Immunol.* 2010;184:1049-61.
56. **Mediero A, Ramkhalawon B, Wilder T, Purdue PE, Goldring SR, Dewan MZ, et al.** Netrin-1 is highly expressed and required in inflammatory infiltrates in wear particle-induced osteolysis. *Ann Rheum Dis* 2016;75:1706-13.

57. **Jain N, Vogel V.** Spatial confinement downsizes the inflammatory response of macrophages. *Nat Mater* 2018;17:1134-44.
58. **Schoon J, Hesse B, Rakow A, Ort MJ, Lagrange A, Jacobi D, et al.** Metal-specific biomaterial accumulation in human peri-implant bone and bone marrow. *S Adv Sci* 2020;7(20):2000412. doi: 10.1002/advs.202000412.
59. **Xu J, Yang J, Chen J, Zhang X, Wu Y, Hart A, Nyga A and Shelton JC.** Activation of synovial fibroblasts from patients at revision of their metal-on-metal total hip arthroplasty. *Part Fibre Toxicol* 2020;17:42 doi.org/10.1186/s12989-020-00374-y.
60. **Ninomiya JT, Kuzma SA, Schnettler TJ, Krolikowski JG, Struve JA, Weihrauch D.** Metal ions activate vascular endothelial cells and increase lymphocyte chemotaxis and binding. *J Orthopaedic Res* 2013;31:1484-491.
61. **Baskey SJ, Lehoux EA, Catelas I.** Effects of cobalt and chromium ions on lymphocyte migration. *J Orthop Res* 2017;35:916-24.
62. **Schmalzried T.** Metal-metal bearing surfaces in hip arthroplasty. *Orthopedics*. 2009;32. DOI:10.3928/01477447-20090728-06.
63. **Langton DJ, Jameson SS, Joyce TJ, Hallab NJ, Nattu S, Nargol AV.** Early failure of metal-on-metal bearings in hip resurfacing and large-diameter total hip replacement: A consequence of excess wear. *J Bone Joint Surg Br.* 2010;92:38-46.
64. **Jennette JC, Falk RJ, Bacon PA, Basu N, Cid MC, Ferrario F, et al.** 2012 revised International Chapel Hill Consensus Conference Nomenclature of Vasculitides. *Arthritis Rheum* 2013;65:1-11.

Figure 1 Histopathological classification of ALTR/ARMD

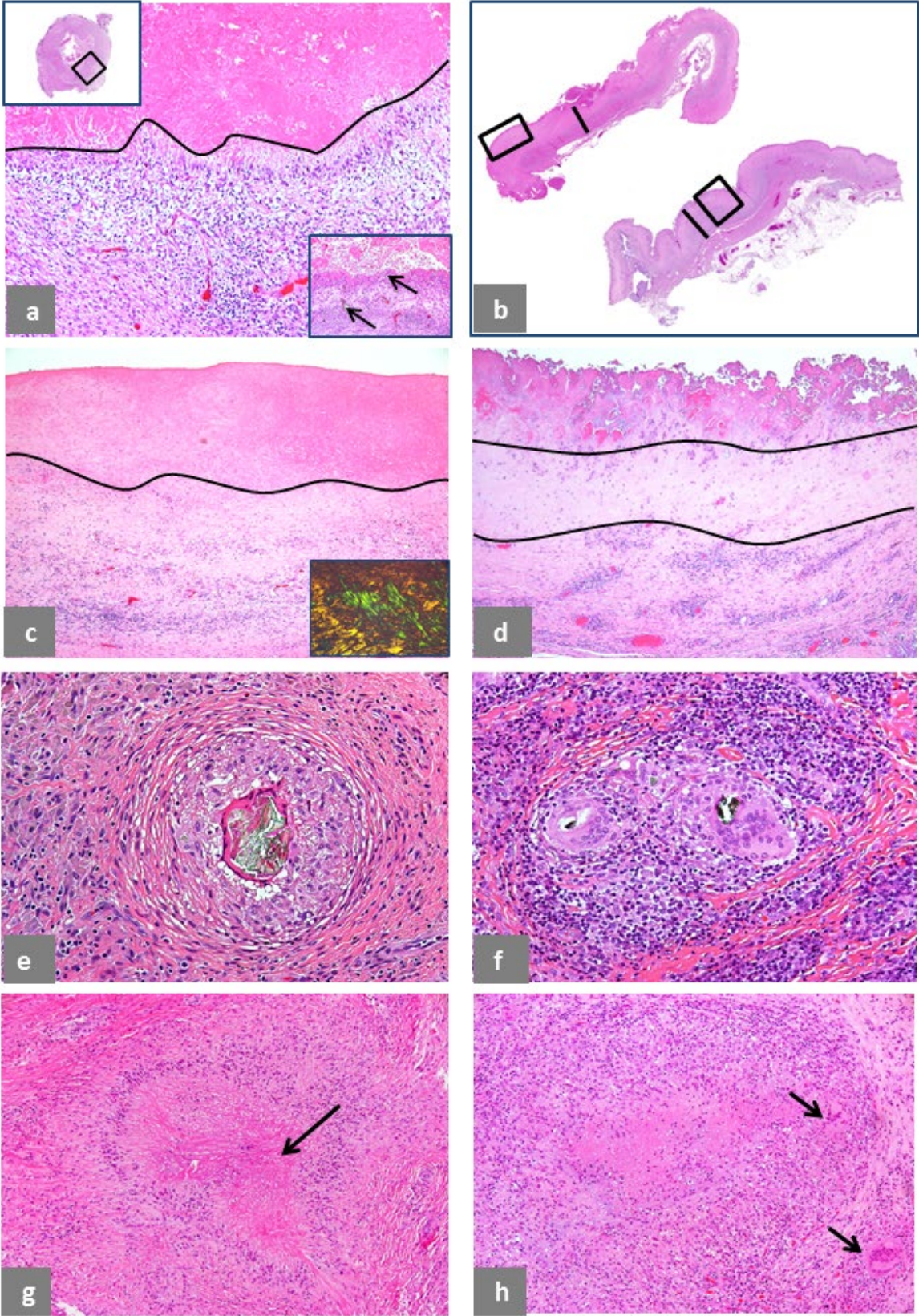


Figure 2 Lymphocytic infiltrate grading

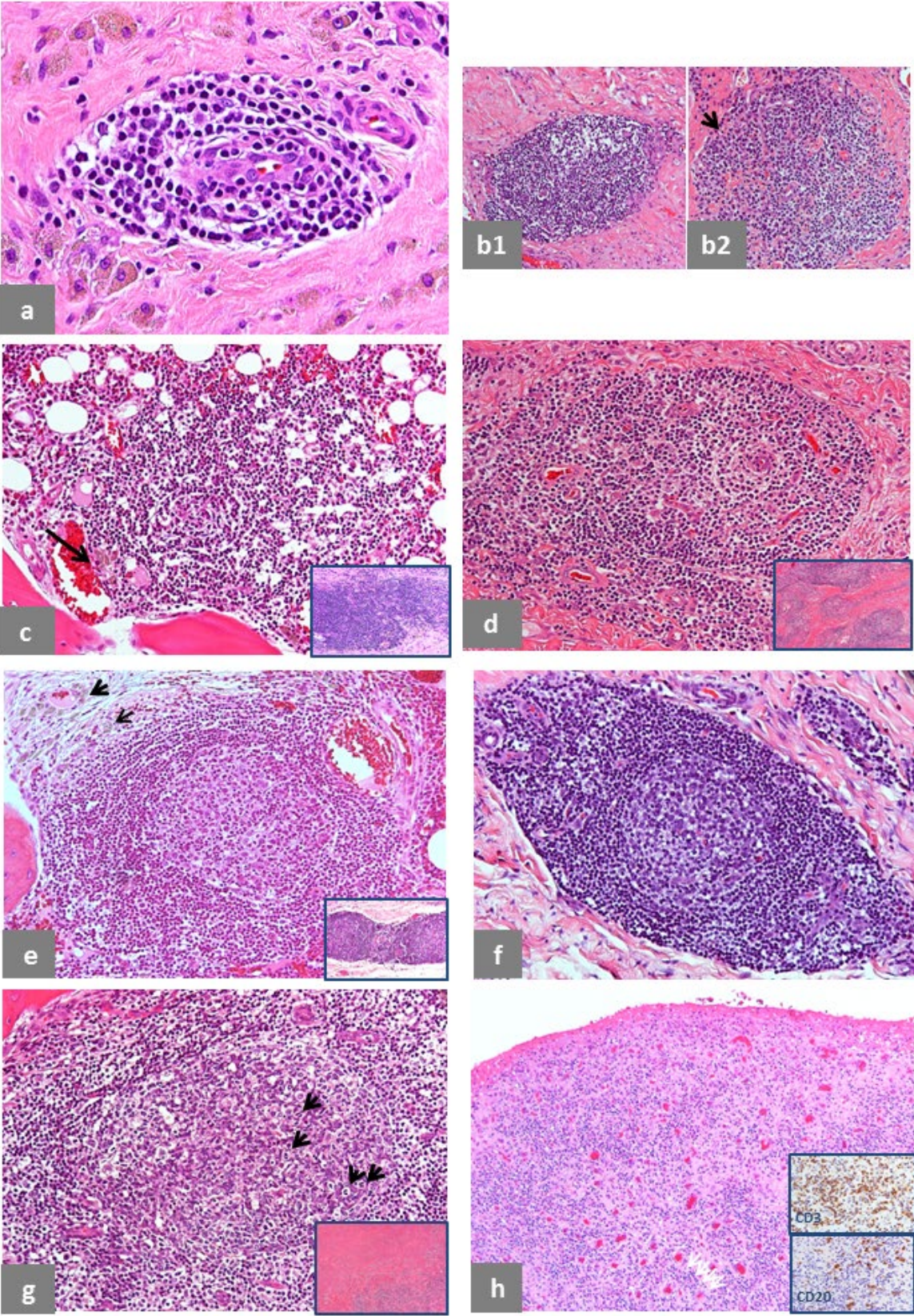


Figure 3 Macrophage infiltrate grade 1, soft tissue and bone marrow

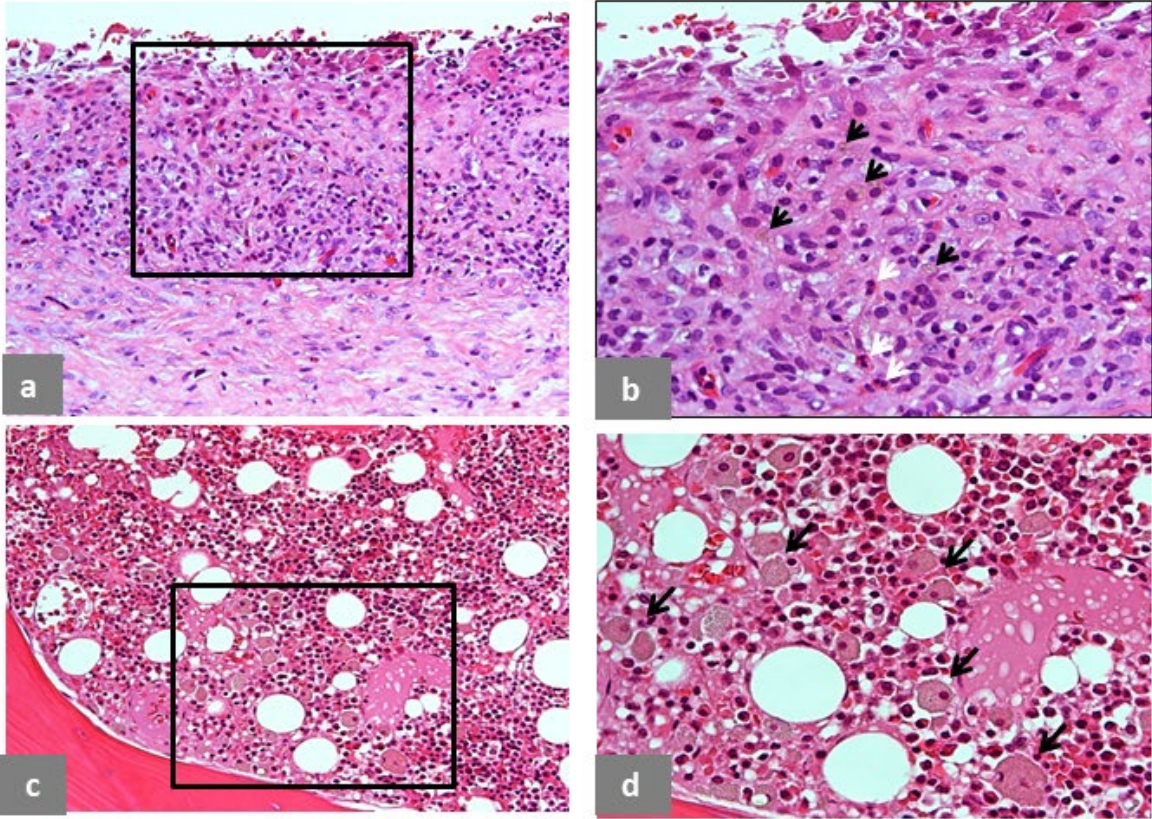


Figure 4 Macrophage infiltrate grade 2, soft tissue

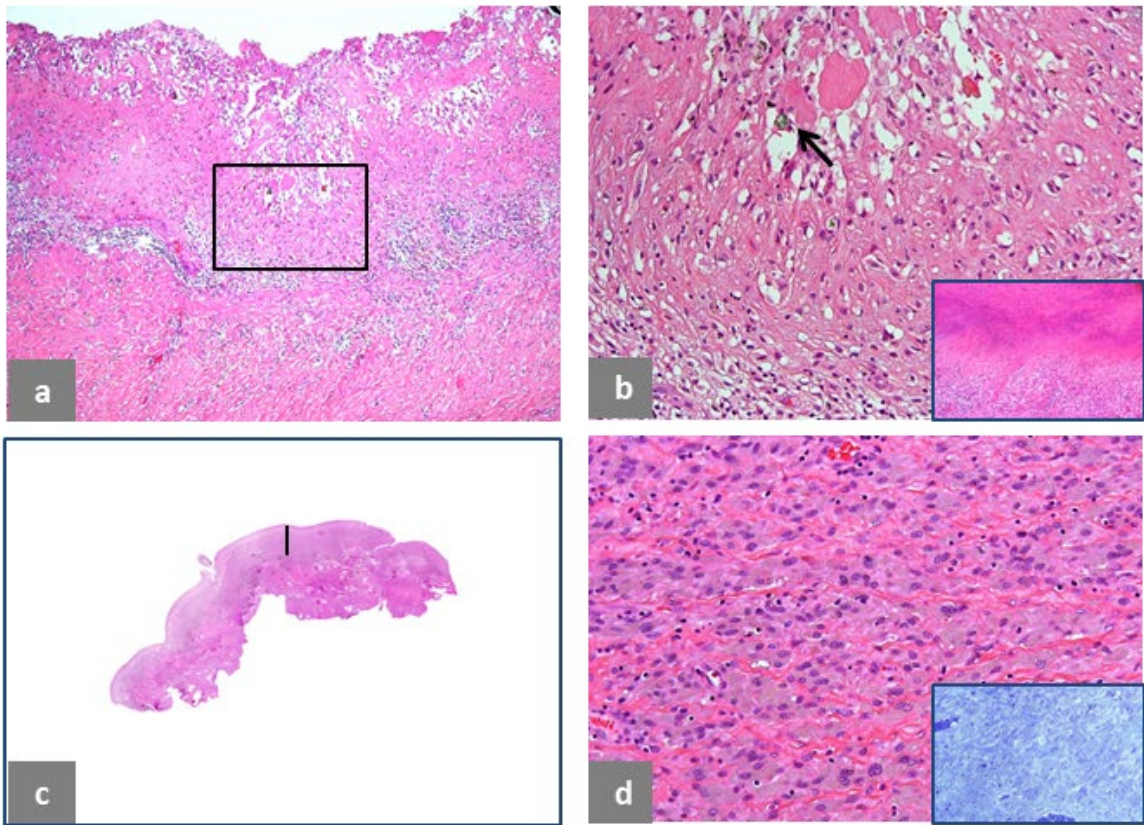


Figure 5 Macrophage infiltrate, soft tissue grade 3, and bone marrow grade 2 and 3

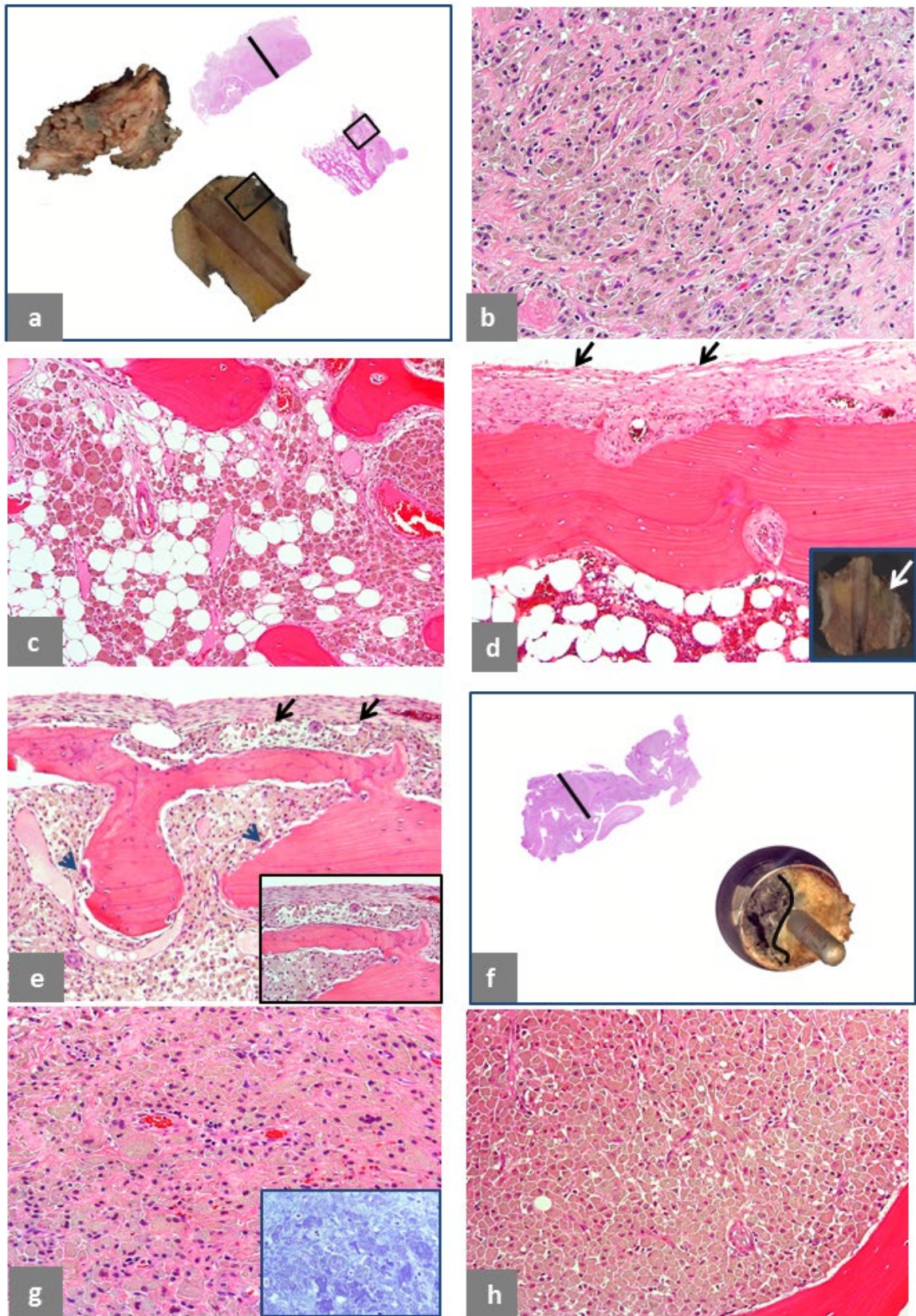


Figure 6 Vascular changes

